Strength of LL Chondrites in Laboratory Deformation Experiments with Applications to Internal Structure of 99942 Apophis

C. Seltzer, M. Pec, H.O. Ghaffari, R.P. Binzel

MIT Department of Earth, Atmospheric, and Planetary Sciences

I. Motivation

As the asteroid 99942 Apophis approaches the Earth in April 2029, it will be subjected to the Earth's gravitational field and experience changes to its internal structure. Here, we conduct laboratory deformation tests on LL chondritic material in order to assess the internal strength and velocity structure of Apophis' component material. These results will allow us to understand what kind of mechanical and seismic outcomes may occur as Apohis passes through the Earth's gravitational field.

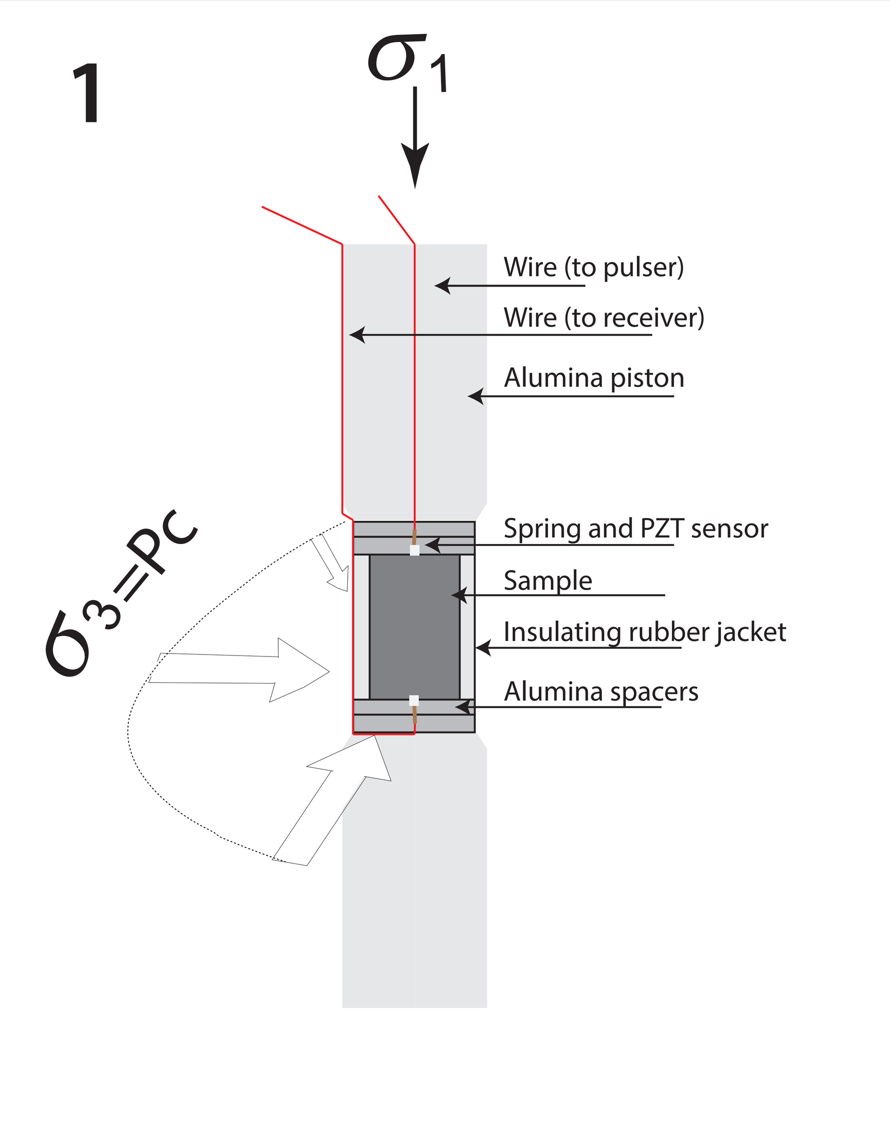

Figure 1: Experimental design

Samples were deformed in a Paterson gas medium deformation apparatus. Each sample was between 7-12mm in length, and had diameters of 6.25mm. Spring-loaded minature sensors were created with a fixed diameter of 1.5mm, and placed above and below the sample to generate and record acoustic waves.

Thank you to the Massachusetts Space Grant Consortium for funding this reasearch.

II. Mechanical Results

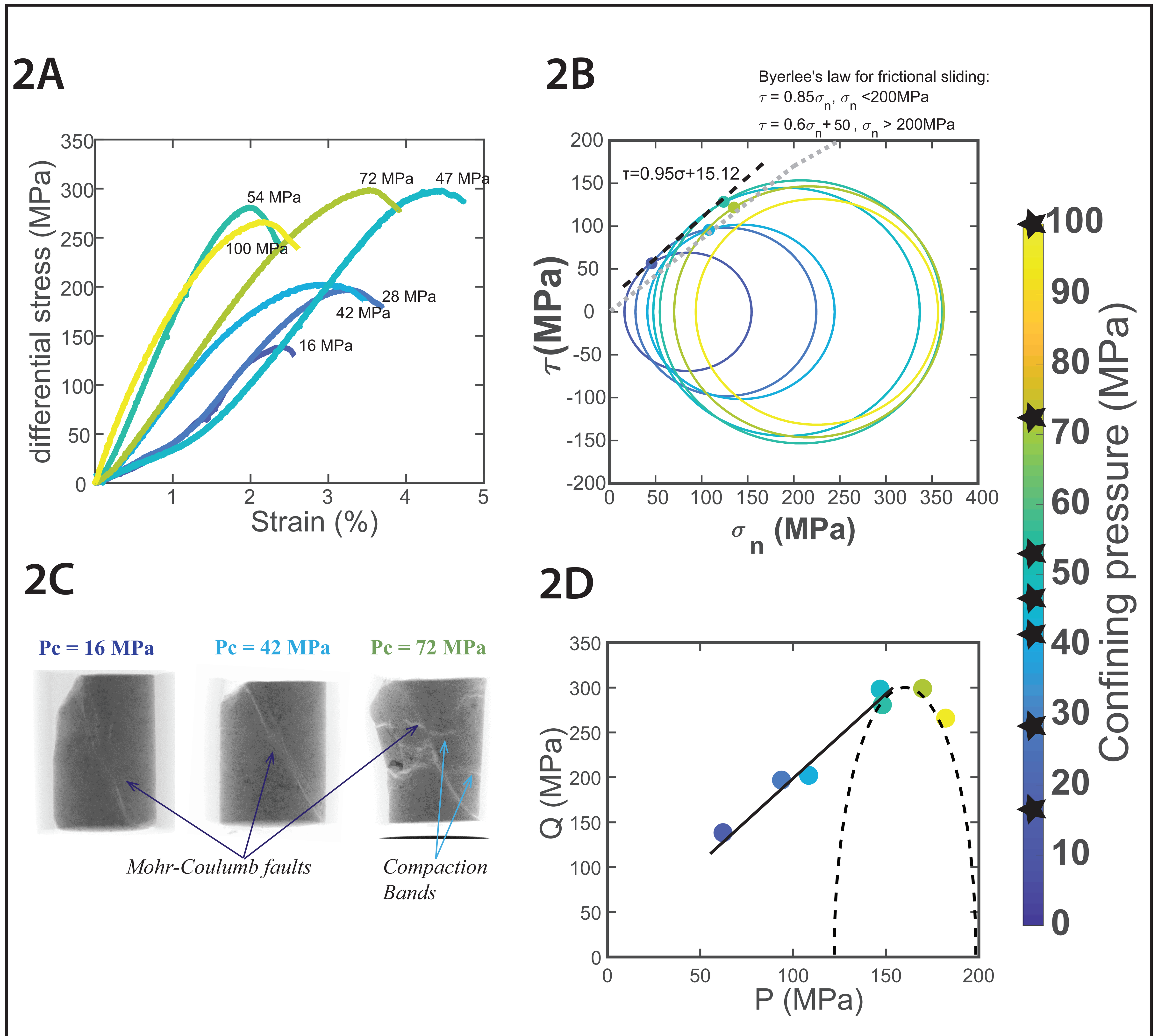

Figure 2: Mechanical results

A. Stress-strain curves for 7 deformation tests. Differential stress is measured as σ_1-σ_3; strain is measured as a % difference in initial and deformed length. Curves are labeled by confining pressure as shown in colorbar to the far right.

B. Mohr Circles for deformed tests. Normal stress, σ_n, is plotted against shear stress, τ, to describe the stress state on all tests at peak strength. Colors correspond to confining pressures. Failure envelope is labeled in black, and Byerlee's law for frictional sliding in grey. Note that the failure envelope falls above Byerlee's law for tests up to 50MPa.

C. Central slices from 3D CT scans of three deformed samples. Each sample exhibits Mohr-Coulumb failure, but only samples above 50 MPa Pc show compaction bands perpendicular to the direction of applied stress.

D. Cap model compaction. Effective mean stress P (σ_1+2σ_3)/3 is plotted against differential stress Q. The point at which the curve turns indicates the beginning of "shear-enhanced compaction", modeled as an ellipse.

Chondritic material may deform similarly to porous Earth rocks
Deformation styles differ above and below ~50MPa Pc

III. Ultrasonic Results

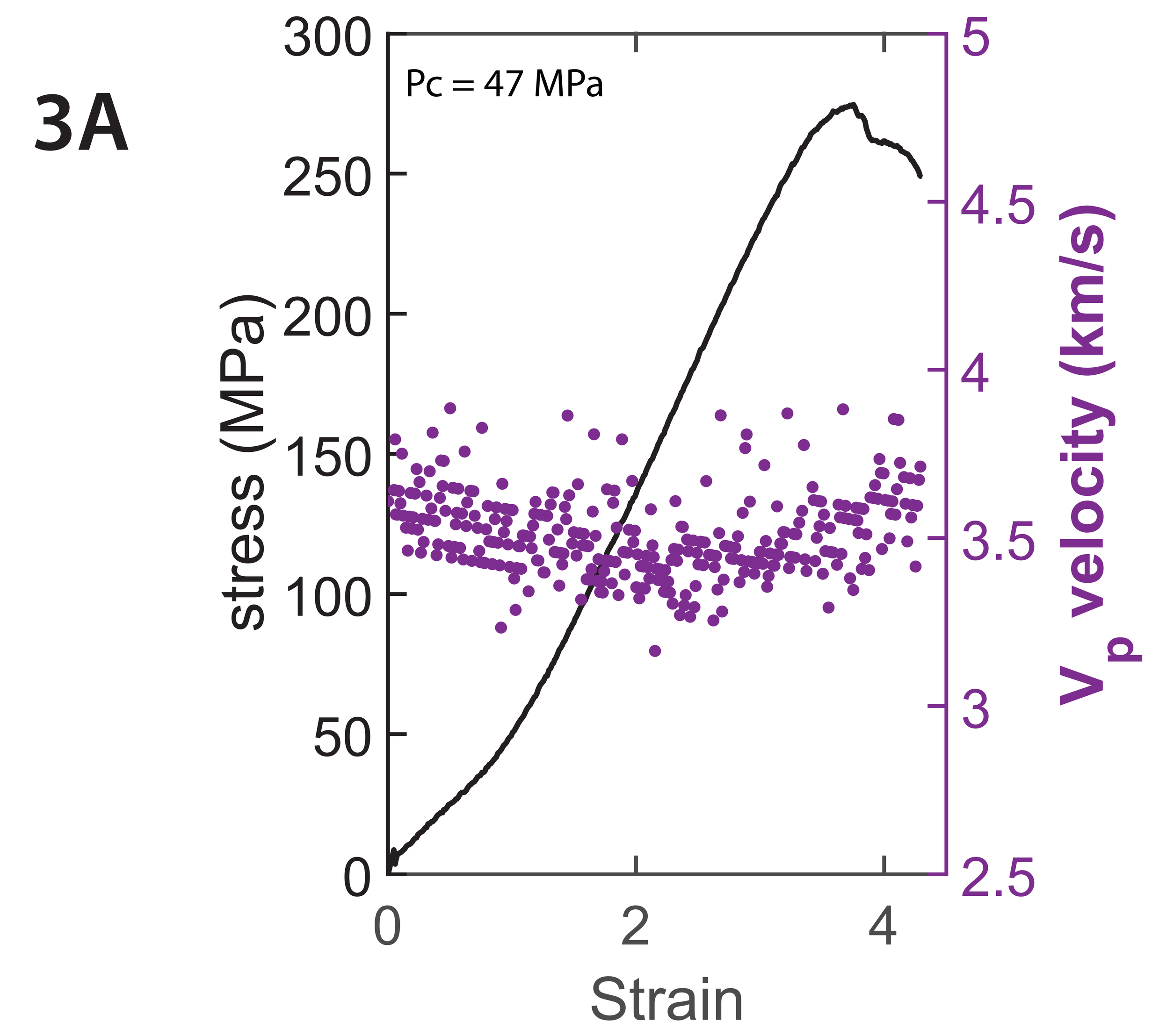

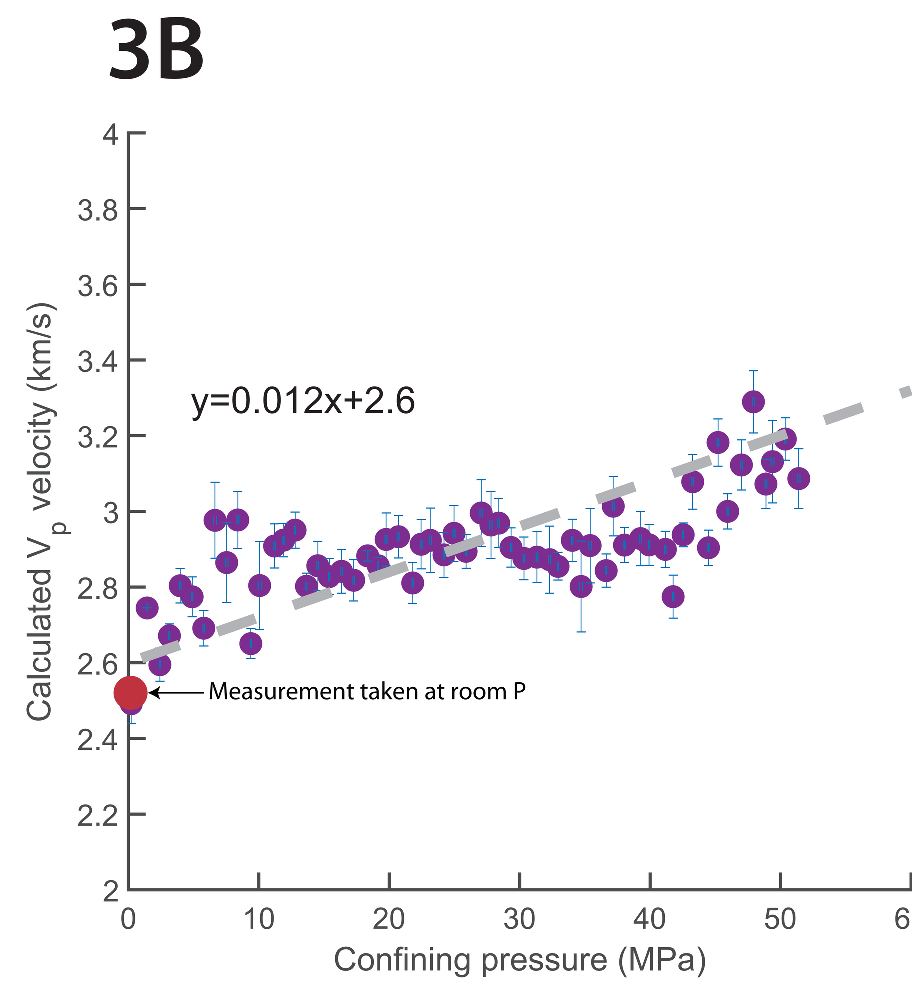

3C

Room condition measurements:

Density $\rho = 3.2 g/cm^3$

$$V_p = \sqrt{\frac{\lambda + 2\mu}{\rho}} = 2.5km/s$$

$$V_s = \sqrt{\frac{\mu}{\rho}} = 1.6km/s$$

Shear modulus $\mu = \rho V s^2 = 8.2GPa$

Bulk modulus $\kappa = \frac{-4}{3}\mu + \rho V p^2 = 9.1GPa$

Poisson ratio $\nu = \frac{3\kappa - 2\mu}{6\kappa + 2\mu} = 0.15$

Young's modulus $E = \frac{9\kappa\mu}{3\kappa + \mu} = 19GPa$

Lame's first parameter $\lambda = \frac{3\kappa - 2\mu}{3} = 3.2GPa$

Figure 3: Wavespeeds

A. Vp velocities for a test deformed at 47MPa Pc plotted over stress-strain curve. Velocities decrease, then increase as damage accumulates. This is contrary to what would be expected, as increased cracking usually decreases wavespeed velocities.

B. Confining pressure vs. Vp velocity. Wavespeeds taken in situ during pressurization to 50 MPa plotted with error bars and a best linear fit, along with a single measurement taken at room pressure before deformation.

C. Calculated elastic moduli for Kilabo, taken from Vp & Vs measurements at room conditions.

Wavespeeds evolve with confining pressure, and decrease slightly with deformation before recovering